Available online at www.sciencedirect.com
ScienceDirect
Acta Materialia 54 (2006) 4221–4228
Acta MATERIALIA
www.actamat-journals.com

Plastic flow softening in a bulk metallic glass

R. Bhowmick, R. Raghavan, K. Chattopadhyay, U. Ramamurty *

Department of Metallurgy, Indian Institute of Science, Sir CV Raman Avenue, Bangalore, Karnataka 560012, India

Received 23 March 2006; received in revised form 17 April 2006; accepted 7 May 2006
Available online 18 July 2006

Abstract

An experimental investigation into the role of the excess free volume that is created during plastic deformation in strain softening of amorphous metals was conducted. A well-defined and large plastic zone was created through the spherical indentation of a bonded interface of a Zr-based bulk metallic glass (BMG). Elastic modulus and hardness mapping of the deformation zone was conducted through nanoindentation. Experimental observations show that the load, P, vs. depth of penetration, h, curves obtained from the deformation zone are decorated with discrete displacement jumps, which are otherwise absent in the undeformed material. The prior-deformed zone underneath the large indenter was also found to be softer than that far away from the indenter. A simple and approximate analysis shows that the strain softening of the BMG is related to the excess free volume that is created during prior deformation. Contrary to general expectation, differential scanning calorimetry of the deformed material indicates a reduced free volume. These results can be explained by postulating the formation of nanovoids due to the coalescence of the excess free volume. These nanovoids, in turn, lower the stress required for plastic deformation through shear bands, which leads to the observation of reduced hardness.

Keywords: Metallic glasses; Plastic deformation; Shear bands; Nanoindentation; Free volume

1. Introduction

Plasticity in metallic glasses is accommodated through the formation of shear bands, facilitated by the creation of free volume during the deformation that leads to local reductions in viscosity [1]. Hajlaoui et al. [2] utilized X-ray diffraction in transmission during heating using synchrotron radiation to study the free volume generated due to deformation of bulk metallic glasses (BMGs) and showed that a 37% increase in free volume was observed during ball indentations of Zr-based metallic glass ribbons. However, theoretical investigations suggest that the excess free volume is not stable. Wright et al. [3] modeled this phenomenon and suggested that thermodynamics favor the coalescence of excess free volume resulting in the formation of voids within the shear bands once the externally applied stress is removed. High-resolution transmission electron microscopy of the shear bands by Li et al. [4] and positron annihilation spectroscopy studies by Flores et al. [5] show that the shear bands contain a high concentration of nanometer-scale voids, whose volume fraction is estimated to be ~0.4%, which is considerable. As a result, the voids are likely to influence the subsequent plastic deformation in a significant manner. For example, Wright et al. [2] suggest that these voids are the reason for the lack of tensile ductility in metallic glasses, as they act as initiators of instability that leads to instantaneous fracture. On the other hand, several studies indicate nanocrystallization in shear bands due to the high intensity of deformation in them [4–6]. Jiang et al. [6] studied the dependence of the nature of the stress state on the plastic flow. They observed voids in the tensile side of a bent Al-based rapidly quenched metallic glass, while there were nanocrystallites in the shear bands along with small cracks in the compression side of the neutral axis.

Either way, these structural evolutions within the deformed region can impart length scale and/or history dependence to subsequent plasticity. For example, the nanovoids can act as nucleation sites for the shear bands

* Corresponding author. Tel.: +91 80 2293 3241; fax: +91 80 2360 0472.
E-mail address: ramu@met.iisc.ernet.in (U. Ramamurty).

1359-6454/$30.00
doi:10.1016/j.actamat.2006.05.011

and hence can enhance the plasticity of BMGs (though in tensile loading nanovoids may lead to cracks and not shear banding). In contrast, nanocrystallization was shown to increase the strength of BMGs [7]. In this paper, we critically assess these possibilities. We employ the bonded interface technique to generate a well-defined deformation region [8]. A large deformed region is created by applying macroscale spherical indentation, for which analytical functions to describe the stress and strain fields underneath the indenter are available. The deformed region, thus produced, is further probed using a nanoindenter. Hardness and modulus maps of deformed as well as undeformed regions (produced through identical experimental steps) are generated and compared.

2. Material and experiments

A $Zr_{41}Cu_{14}Ti_{12}Ni_{10}Be_{23}$ BMG (referred to as Vit1) obtained in the form of a 3 mm thick plate was used for the present study. Specimens for the bonded interface technique were prepared by cutting the plate specimen first into two halves and then polishing them to a 1 μm finish prior to bonding them using a high-strength adhesive. Following this, the top surface of the bonded specimen was polished so that it was flat. Spherical indentations with loads ranging between 100 and 500 N were performed using a 2 mm diameter WC sphere such that the diameter of the indenter impression coincided with the interface. The bonded interface was opened subsequently, by dissolving the adhesive in acetone, and the subsurface deformation zone was examined using scanning electron microscopy (SEM). The spatial coordinates of the deformed region were identified with the aid of four large Vickers indents (serving as reference points) made at the corners of the deformed regions. After this, the surface protrusions were gently polished off (in order to have a smooth surface necessary for nanoindentation) using diamond paste (<0.25 μm).

Nanoindentation experiments were conducted using a Hysitron Triboindenter on the deformed region as well as away from it. The P–h curves obtained were corrected for any drift through auto-calibration before each indentation experiment was performed. A 25 μm distance (in both directions) between each indent was maintained. The first row of indents was a distance of 20 μm away from the free surface. A maximum load of 5 mN with a loading rate of 0.5 mN/s (with a 5 s hold time at the peak load) was applied. Measurements far way from the deformed region (referred to as 'bulk') were also conducted for comparison purposes. Selected indents were imaged using the indenter tip itself in the direct contact mode of atomic force microscopy (AFM). SEM was used to image the other indents.

For differential scanning calorimetry (DSC) experiments, slices of approximately 500 μm were cut using a low-speed diamond saw from the as-cast BMG samples. The slices were then mechanically polished to 300 μm and indented with a spherical indenter using a load of 625 N. The spherical impressions were produced so as to touch each other and covered the surface area completely. These deformed samples were cleaned using acetone and scanned using a Mettler Tolledo 822^e DSC instrument at a rate of 0.333 K/s. In the undeformed case, the samples were scanned after thinning down to 300 μm.

3. Results

3.1. Deformation morphology

Fig. 1 shows the morphology of the deformed region underneath the spherical indenter (load = 300 N). Just below the indent tip an elastic zone with a width of ~35 μm that is devoid of any shear bands is seen (shown in the inset). Beneath it, a semicircular deformation zone containing a high density of shear bands with two types of bands, semicircular and radial, is present. The semicircular bands are a result of the out-of-plane plastic flow of the BMG (into the compliant interface), corresponding to plane-stress deformation conditions [8]. The radial bands are a result of plane-strain deformation. The average intersection angle between the radial bands is 101.2°, implying pressure sensitivity to plastic deformation [9]. Fig. 2 shows a plot of the interband spacing, λ, as a function of radial distance away from the indenter tip, L. Despite the large scatter in λ (ranging between 2 and 25 μm with an average value of ~9 μm), a curve fitted through the entire data indicates that there is a slight decrease in λ between 60 and 140 μm away from the free surface, implying extensive plastic deformation in this region.

3.2. Nanohardness

The average elastic modulus, E, and hardness, H_0, of the undeformed material measured using nanoindentation are 114 and 7.1 GPa, respectively. The value of E is consistent with that of Wright et al. [10] who conducted nanoindentation experiments using Vit1. However, it is ~17.5% larger than the value of E measured in uniaxial tests [11]. Similarly, H is also ~18% larger than the literature value. These

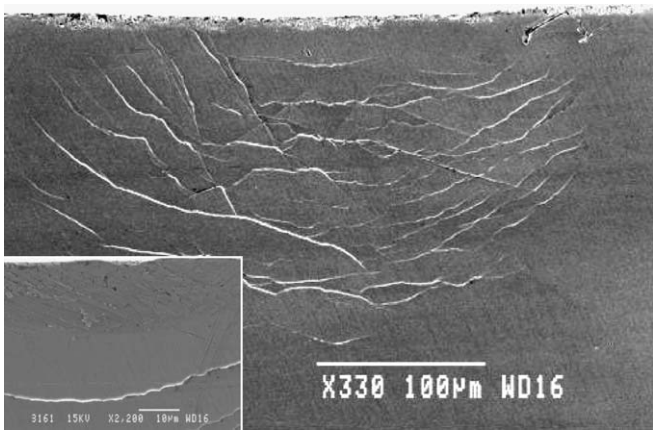

Fig. 1. Subsurface deformation morphology under a spherical indenter. Inset shows the elastic zone immediately beneath the indenter tip.

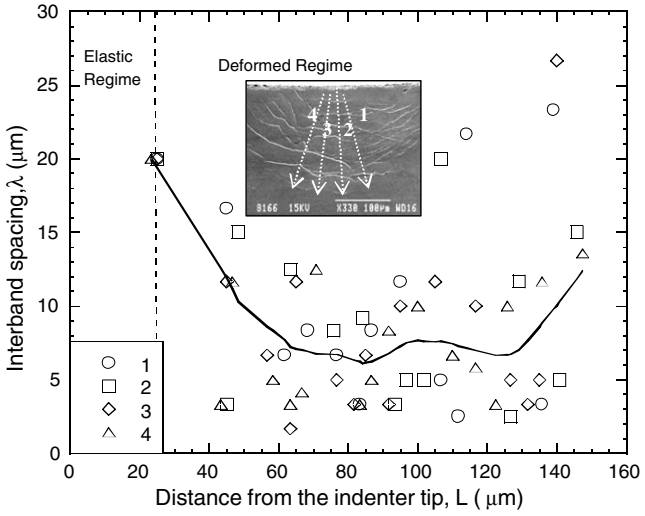

Fig. 2. Interband spacing as a function of distance from the indenter tip. Inset shows the directions along which the interband spacings have been measured.

discrepancies are due to extensive pile-up observed which results in an underestimate of the indented area. The contour map of the hardness values measured through nanoindentation (Fig. 3) indicates a softer kidney bean-shaped region beyond the elastic zone. The variation of H (normalized with respect to the bulk hardness value, H_0) with L is plotted in Fig. 4(a), which shows that H/H_0 is similar to the bulk values close to the indenter tip (within the elastic region). However, the hardness of the extensively deformed region is lower, ranging between 6.2 and 6.6 GPa. The difference between the lowest H measured in the soft region and that measured for the bulk is 16%, which is much larger than the experimental scatter. To further confirm that the hardness changes observed are not artifacts of the experimentation (because of the changes in the contact area due to plastic flow and pile-up of the material around the indenter), the variation of H/E^2 is plotted against L in Fig. 4(b). (Note that E is not expected to change significantly with free volume. However, E estimated using the

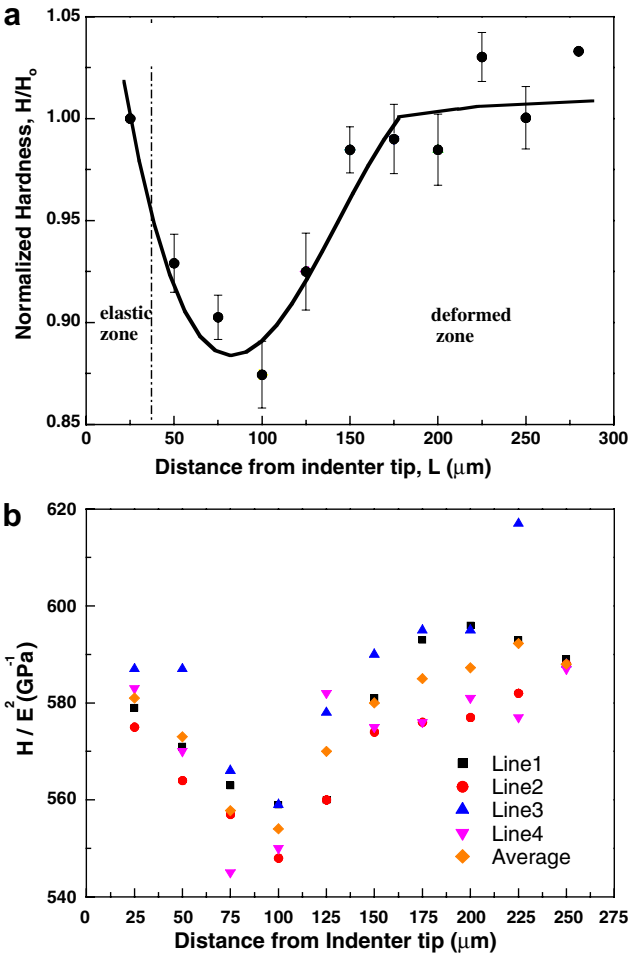

Fig. 4. (a) Variation of hardness with the radial distance from the indenter tip. (b) Variation of H/E^2 with the radial distance from the indenter tip.

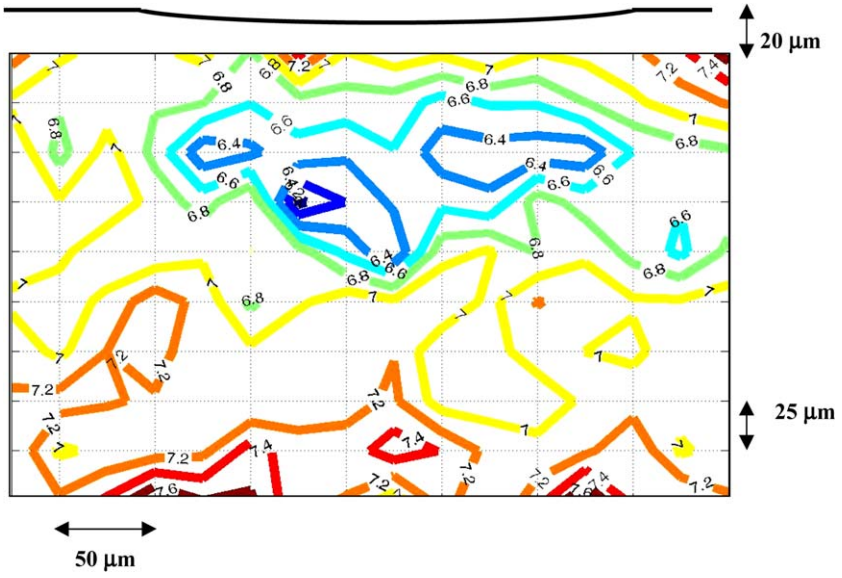

Fig. 3. Hardness contours, obtained from the nanoindentation experiments, within the deformed region.

Oliver and Pharr method [12] would not account for the pile-up. Since E depends on the square root of the area, H/E^2 should reflect the actual changes in hardness.) This plot shows a similar variation to that of H/H_0 with L (Fig. 4(a)), indicating that the observed softness is indeed a reflection of the material condition.

3.3. P–h curves

A series of P–h curves generated using nanoindentation along the central axis of the deformed region leading towards the indenter tip are shown in Fig. 5(a). The P–h curves generated either in the elastic region immediately beneath the indenter or in the bulk are relatively smooth with the magnitude of serrations being less than 1 nm. In contrast, the P–h curves generated within the deformed region are decorated with large displacement jumps, $h_{\text{pop-in}}$, which range between 4 and 7.3 nm with an average of ~4.8 nm. Results of nanoindentation of BMGs reported in the literature show that the pop-ins in the P–h curves are due to the nucleation and propagation of shear bands underneath the indenter [10,13,14]. Schuh and Neih [14] mention that the P–h curves obtained for Zr-based BMGs are relatively smooth compared to those observed in Pd-based BMGs, consistent with the P–h curves obtained from the undeformed region (that is, immediately below the spherical indenter tip) as well as from the bulk. Murali and Ramamurty [15] observe that in Vit1 the $h_{\text{pop-in}}$ measurements could not be made for h below ~200 nm as serrations are difficult to resolve. These observations imply that the displacement jumps in the P–h curves obtained from the deformed region are a result of the shear banding-induced structural changes.

SEM images (Fig. 5(b)) of the indents show enhanced contrast surrounding those obtained from the deformed region, implying larger pile-up of the material at the edges. Plastic flow in non-strain hardening materials like BMGs occurs against the faces of the indenter due to the incompressibility of the plastic deformation and results in pile-up. Fig. 6(a) shows a line scan across an indent (made in the bulk) that confirms large pile-up around the indents. The pile-up can be quantified through the ratio of h_r, the residual depth, to the maximum depth achieved during the indentation, $h_{\max}$ [16]. The higher the value of $h_r/h_{\max}$, the greater is the extent of pile-up. A plot of $h_r/h_{\max}$ (normalized with that obtained in the elastic region) as a function of L in Fig. 6(b) shows that $h_r/h_{\max}$ in the deformed regime is a maximum. Note that the spacing between the shear bands is correspondingly a minimum in the same region (Fig. 2).

4. Discussion

4.1. Excess free volume

Recent indentation studies have shown that the plasticity in BMGs is pressure sensitive [9,17]. Lu and Ravichandran [18] studied the plastic deformation behavior of Vit1

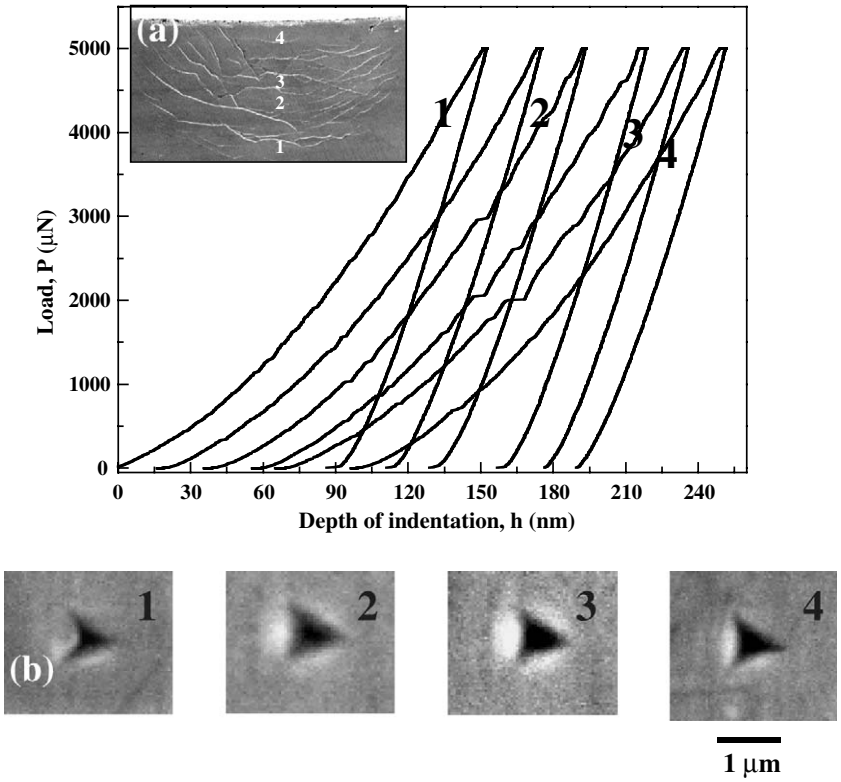

Fig. 5. P–h curves for a series of nanoindents leading to the indenter tip. Location of the indents is illustrated in the inset. (b) SEM images of the corresponding nanoindents.

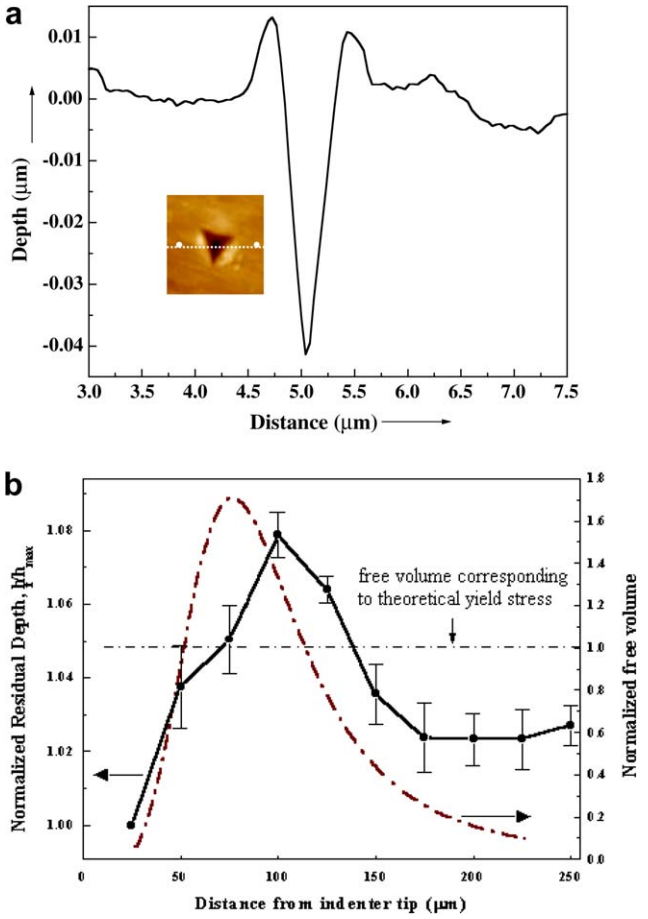

Fig. 6. (a) Line scan across an indent showing the pile-up at its edges. (b) Plot of pile-up as a function of distance from the indenter tip. The amount of free volume generated due to the indentation stress is also shown.

using confined compression experiments and suggested that the plastic flow in it is governed by a pressure-dependent Tresca criterion of the following type:

$$\sigma_y(p) = \sigma_{y,0} - \beta p \tag{1}$$

where $\sigma_{y,0}$ is the flow stress under uniaxial loading, p is the hydrostatic pressure and β is the coefficient of pressure dependence (~0.17 for Vit1). Combining this with the analytical expressions available for the distribution of stresses in Hertzian contact [19], the variation of shear stress, τ, as a function of depth is obtained, which shows that just below the indenter (for about 40 μm) the stress is less than the yield stress and hence an elastic zone exists.

For the case of steady-state inhomogeneous flow, Spaepen [1] derived the following relationship between the free volume, v_f, and shear stress, τ:

$$\gamma \frac{v^*}{v_f} = \frac{v^*}{n_D} \frac{S}{2kT} \left[\cosh\left(\frac{\Omega}{2kT} \tau \right) - 1 \right]^{-1} \tag{2}$$

where γ is the macroscopic shear strain, Ω is the atomic volume, v^* is the hard sphere equivalent of the atomic volume, S is a constant derived from the Eshelby model, and k and T are the Boltzmann constant and absolute temperature, respectively. With the knowledge of τ as a function of z, the variation of normalized free volume (with respect to that at the yield stress of 1.92 GPa) with the distance away from the indenter tip is obtained (Fig. 6(b)). The trends in pile-up and excess free volume are similar, implying that the strain softening observed in the prior-deformed region is due to the generation of free volume during the indentation process.

It is important to note here that we have used the free volume model of Spaepen for the sake of simplicity. Recently, many observations/models that capture the essence of plasticity in amorphous alloys have been made and we discuss them here briefly in order to put the current work in proper perspective. Novikov and Sokolov [20] have observed that the fragility (an indicator of how the viscosity of the glass changes through the glass transition and in turn the glass-forming ability of a liquid) is intimately connected to Poisson's ratio, which depends on the shear and bulk moduli ratio. In a similar vein, Johnson and Samwer [21] have observed that the shear strain at yield, γ_c (given by the shear strength to the shear modulus ratio), typically is ~2.67%. Further, they observed that γ_c is inversely proportional to the glass transition temperature, T_g. On the basis of these observations, Johnson and Samwer [21] proposed a model for explaining plastic deformation in metallic glasses, which is based on the shear transformation zone (STZ) theory proposed by Argon [22]. Using Frenkel's [23] approach to calculate the theoretical strength of dislocation-free crystals, the concept of the potential energy landscape and inherent states [24] and scaling analysis, they derived a universal law which shows that the shear strength of metallic glasses at a given temperature of testing scales with $T_g^{-2/3}$ [21].

With respect to the stress–strain behavior of BMGs and its dependence on the temperature and the rate of testing, Lu et al. [25] investigated the deformation behavior of Vit1 in the temperature range 283–683 K and strain rate range 10^{-5} to $10^{3}\ s^{-1}$ and noted that the deformation in BMGs can be divided into three regions: (a) Newtonian flow (occurring above 600 K, i.e., in the supercooled liquid region and typically at low strain rates ~$10^{-5}\ s^{-1}$); (b) non-Newtonian flow (at moderate temperatures and strain rates, for example between 550 and 600 K for the strain rate range 10^{-5} to $10^{-4}\ s^{-1}$); and (c) linear elastic deformation followed by shear localization (at temperatures below ~500 K and at relatively higher rates of deformation). The three regimes can be understood in terms of the competition between free volume creation and annihilation (structural relaxation) rates. While the relaxation rate dominates the Newtonian flow region, creation and annihilation of free volume essentially occur at same rate during the non-Newtonian flow. In the case of the low-temperature deformation region of shear localization, the rate of creation of free volume is much larger than that of relaxation, leading to excess free volume. Johnson et al. [26] developed a self-consistent dynamic free volume model that takes into account free volume creation (through the free volume model of the glass transition) and the Vogel–Fulcher–Tamann equation (that

describes the relaxation kinetics in glasses over a wide viscosity range). This model captures the transition from steady-state to non-steady-state flow during shear localization. In the context of the present paper, Lu et al. [25] note that the deformation through shear localization is essentially insensitive to the strain rate. The indentation tests reported in the present paper were always conducted at ambient temperature (~300 K), so shear localization is the dominant mode of plastic deformation. Further, strain rate affecting the observed results can also be ruled out, as per the observations of Lu et al. [25].

4.2. Nanocrystallization in shear bands

Kim et al. [27] reported nanocrystallization in the deformed regions surrounding a nanoindent in a Zr-based BMG, implying that crystallization can occur even under quasi-static loading conditions as a consequence of the dynamic flow dilatation in actively deforming bands with an accompanying enhancement in the atomic mobility through diffusion. However, more recent experimental results of Lewandowski and Greer [28] clearly demonstrate that temperature rise in the shear bands can be as high as a few thousand kelvin over few nanoseconds. Further, they show that that the adiabatic heating does not control the shear band thickness, i.e., it may only play a role in the initiation of shear localization. Yang et al. [29] have proposed a model that shows that shear softening occurs due to both an increase in free volume and an increase in temperature in the shear bands. More recently, Demetriou and Johnson [30] have further extended the work of Johnson et al. [26] through finite element simulations of flow transport to examine the possibility of crystallization during shear flow of BMGs. By considering the enhanced atomic diffusion (due to the excess free volume created) and altered thermodynamics of the system (through non-equilibrium phase separation caused by the shear flow), they show that the TTT (time–temperature-transformation) curve takes an 'S' shape, which implies that the critical cooling rate required no longer depends on the 'nose' of the curve. This implies that crystallization is possible within the shear bands.

Gu et al. [31] reported the presence of closely spaced shear bands in the nanocrystalline region, indicating that, although the nanocrystals may be too small to impede shear band propagation, they may act as initiation sites for shear bands. Although multiplication of shear bands due to uniformly distributed nanocrystals has been used to explain the increase of strength of Zr-based nanocrystalline amorphous alloys [32], no such hardening is observed in the present study. This could be due to either a relatively small size (which leads to engulfment by a moving shear band [33]) or low volume fraction. To further investigate the aforementioned possibilities, we conducted DSC experiments on the deformed material as well as the undeformed material (i.e., as-cast condition). Note that the samples for the DSC scans were prepared in an identical manner as formerly, except for the inducement of plasticity in the former case. Further, we conducted five DSC scans for each case, so as to ascertain the reproducibility and reliability of the DSC results. Representative DSC scans are shown in Fig. 7 and data obtained are summarized in Table 1.

4.3. Calorimetry

Fig. 7 shows that the DSC scans are essentially identical. As seen from Table 1, the crystallization enthalpies at T_g and T_x do not change with deformation. However, an 11.5% reduction in the enthalpy at the glass transition ΔH (calculated by integrating the heat flow, q, between the temperatures of 573 and 653 K) of the deformed glass is noted. Likewise, a reduction of ~20% in the peak value of the heat flow curve before the onset of glass transition is also noted for the deformed glass.

It has been well established in the literature that a direct correlation exists between the enthalpy at glass transition and free volume. Van den Beukel and Sietsma [34] developed a model that describes the functional form of the DSC curves based on free volume theory. According to their model, for every supercooled liquid there exists an equilibrium free volume, v_{fe}, at a given temperature, which is given by the equation

$$v_{fe} = A(T - T_0) \tag{3}$$

where T_0 is the ideal glass temperature and A is a proportionality constant. In the as-cast alloy an excess amount of free volume, $v_f > v_{fe}$, is frozen in due to the non-equilibrium processing conditions, which during continuous heating in a DSC experiment annihilates and approaches v_{fe}. The reduction in v_f gives rise to heat release, ΔH, when the glass sample is heated in a DSC experiment. It was experimentally verified by Slipenyuk and Eckert [35] that

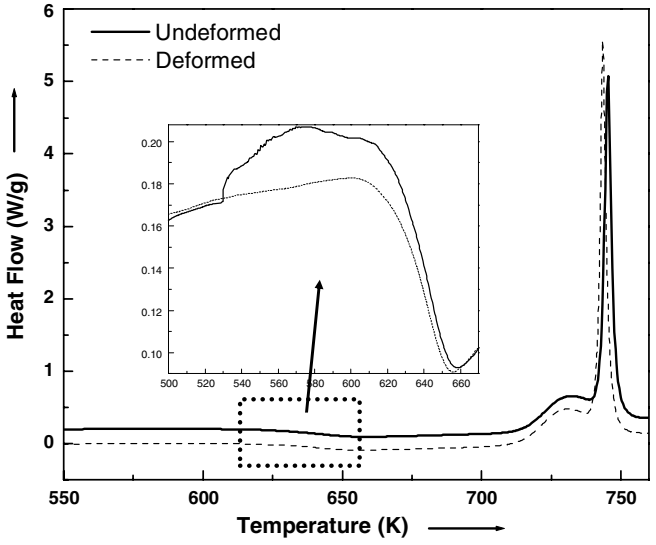

Fig. 7. DSC scans obtained for the undeformed (i.e., as-cast condition) and the deformed Vit1 glass. Inset shows the region near the glass transition temperature.

Table 1
Summary of the DSC results obtained for the as-cast and deformed samples

Condition	Enthalpy at the glass transition (J/g)	Heat flow peak value before T_g (W/g)	Crystallization enthalpy (J/g)	Glass transition temperature[a], T_g (K)	Onset temperature for crystallization, T_x (K)
As-received	6.945 ± 0.626	0.127 ± 0.008	75.132 ± 0.694	642.5 ± 2.33	742.8 ± 0.29
Deformed	6.1425 ± 0.044	0.102 ± 0.014	75.312 ± 1.302	643 ± 0.93	742.4 ± 0.48

[a] Inflection point.

$$\Delta H \propto \Delta v_f. \quad (4)$$

The exothermic peak seen before the glass transition is the result of annihilation of excess free volume, Δv_f. Hence, it is possible to estimate the relative changes (due either to heat treatments or to deformation) in the free volume by monitoring ΔH [15]. Here, we use this principle to study the deformation-induced free volume change, with the following logic. If there is an increase in the free volume with deformation, the DSC experiments should yield a higher enthalpy at the glass transition in the deformed glass compared with the as-received glass. However, experimental results presented in Table 1 indicate a definite reduction in ΔH, which implies that there is a reduction in free volume due to deformation. This observation, on the face of it, is contrary to the expectation that excess free volume is generated during deformation.

4.4. Nanovoid formation

We consider the following three reasons for possible explanation: (1) the excess free volume is condensed into nanovoids; (2) the excess free volume helps the process of diffusion for atoms to rearrange and form nanocrystallites, thus effectively reducing the free volume; and (3) both processes (1) and (2) take place simultaneously. Also, the strain (which is much higher than in tension or compression testing) that induces adiabatic heating [28] may aid both processes by increasing the diffusivity of the free volume or rearrangement of atoms as the case might be.

The fact that neither the crystallization enthalpy nor T_x change with deformation implies that nanocrystallization induced by deformation may not be a major factor. In the case where the nanocrystallites were present, they would have acted as precursors to crystallization and hence the whole glass transition process should have been affected. These observations are consistent with those of Kramer et al. [36], who critically examined the possibility of nanocrystallization during cylindrical indentation. No significant structural difference (evaluated using a high-energy X-ray beam) between the deformed and undeformed zones under an indentation was noted. The small shift in the peaks found by Kramer et al. [36] is attributed to deformation-induced free volume change. They milled out a shear band from the deformed zone using a focused ion beam instrument and did not find any crystallization from transmission electron microscopy observations. Because the indent was formed by pressing the curved surface of a cylinder onto the sample, Kramer et al. [36] showed that the maximum pressure below the indenter is at least an order of magnitude lower than that required to induce crystallization, as evidenced in other studies.

Therefore only the first process, i.e., condensation of the excess free volume generated during prior-plastic deformation into nanovoids, appears to be a strong possibility. The formation of nanovoids may lead to a net reduction in the free volume in the material. Observation of a lower ΔH from the DSC scans supports this. These voids may be favorable sites for shear band nucleation during subsequent nanoindentation. The relatively large pop-ins observed in the P–h curves support this argument.

4.5. Plastic softening

Plastic softening induced by deformation processes such as compression, rolling, milling, etc., in different metallic glass alloys has been recently reported [37–39]. Safarik et al. [37] observed a significant reduction in the enthalpy at the glass transition upon deformation. The deformed DSC samples were obtained from regions subjected to maximum shear within a compression-tested sample. For comparison purposes, samples from the same compression-tested sample, but subjected to minimal shear were scanned using DSC. Jiang et al. [38] report a reduction in the nanohardness of a rolled Al-based glassy alloy and attribute it to the presence of retained excess free volume after nanovoid formation in the rolling-induced shear bands. The pre-existing shear bands form weak links and are preferred sites for further deformation. In situ experiments by Yavari et al. [39] have shown that the free volume in deformed metallic glass ribbons is twice that in the as-cast state. They have calculated the densification of deformed and as-cast metallic glass ribbons on heating through the glass transition temperature using in situ X-ray diffraction in transmission. They argue that, unlike crystals, vacancies or atom-sized holes are unstable in glasses and hence the average interatomic volume scales with the macroscopic sample dimensions.

These results and suggested mechanisms are consistent with the observations of the present study.

5. Summary and conclusions

The bonded interface technique is employed to generate a well-defined plastic deformation region through spherical indentation in a Zr-based BMG. This extensive shear banded region was investigated for its mechanical response

through subsequent nanoindentation, which shows that it has lower hardness. Further, the *P–h* curves obtained from within this region are decorated with relatively large displacement bursts. Through an approximate analysis, it has been shown that the normalized residual depth, an indicator of the relative ease with which a material can plastically deform, is correlated with the excess free volume that is created due to deformation. Further, DSC analysis of the deformed region shows that there is a definite decrease in the free volume of the glass after deformation. These observations suggest that the nanovoids formed, due to the coalescence of the excess free volume that is generated during prior plastic deformation, could be the reason for the observed serrations in the *P–h* curves obtained with nanoindentation and the lower hardness of the deformed region.

Acknowledgements

The authors acknowledge the support of Mr. G. Ramakrishna in the nanoindentation experiments and Mr. P. Murali for discussions on this topic. Invaluable inputs and encouragement of Prof. W.D. Nix, Stanford, California, are gratefully acknowledged. Financial support for this work was provided by a grant from the Defence Research and Development Organization, Government of India.

References

[1] Spaepen F. Acta Metall 1975;25:407.
[2] Hajlaoui K, Benameur T, Vaughan G, Yavari AR. Scripta Mater 2004;51:843.
[3] Wright WJ, Hufnagel TC, Nix WD. J Appl Phys 2003;93:1432.
[4] Li J, Wang ZL, Hufnagel TC. Phys Rev B 2002;65:144201.
[5] Flores KM, Suh D, Asoka-Kumar P, Sterne PA, Howell RH, Dauskardt RH. J Mater Res 2002;17:1153.
[6] Jiang WH, Atzmon M. Scripta Mater 2006;54:333.
[7] Leonhard A, Xing LQ, Heilmaier M, Gerbert A, Eckert J, Schultz L. Nanostruct Mater 1998;10:805.
[8] Jana S, Ramamurty U, Chattopadhyay K, Kawamura Y. Mater Sci Eng A 2004;375–377:1191.
[9] Patnaik MNM, Narasimhan R, Ramamurty U. Acta Mater 2004;52:3335.
[10] Wright WJ, Saha R, Nix WD. Mater Trans JIM 2001;42:642.
[11] Bruck HA, Christman T, Rosakis AJ, Johnson WL. Scripta Metall Mater 1994;30:429.
[12] Oliver WC, Pharr GM. J Mater Res 1992;7:1564.
[13] Golovin YI, Ivolgin VI, Khonik VA, Kitagawa K, Tyurin AI. Scripta Mater 2001;45:947.
[14] Schuh CA, Nieh TG. Acta Mater 2003;51:87.
[15] Murali P, Ramamurty U. Acta Mater 2004;53:1467.
[16] Pharr GM. Mater Sci Eng A 1998;253:151.
[17] Vaidyanathan R, Dao M, Ravichandran G, Suresh S. Acta Mater 2001;49:3781.
[18] Lu J, Ravichandran G. J Mater Res 2004;18:2039.
[19] Johnson KL. Contact Mechanics. Cambridge, UK: Cambridge University Press; 1985.
[20] Novikov VN, Sokolov AP. Nature 2004;431:961.
[21] Johnson WL, Samwer K. Phys Rev Lett 2005;95:195501.
[22] Argon AS. Acta Metall 1979;27:47.
[23] Frenkel J. Z Phys 1926;37:572.
[24] Debenedetti PG, Stillinger FH. Nature 2001;410:259.
[25] Lu J, Ravichandran G, Johnson WL. Acta Mater 2003;51:3429.
[26] Johnson WL, Lu J, Demetriou MD. Intermetallics 2002;10:1039.
[27] Kim JJ, Choi Y, Suresh S, Argon AS. Science 2002;295:654.
[28] Lewandowski JJ, Greer AL. Nature Mater 2006;5:15.
[29] Yang Q, Mota A, Oritz M. Comput Mech 2006;37:194.
[30] Demetriou MD, Johnson WL. Acta Mater 2004;52:3403.
[31] Gu X, Livi KJT, Hufnagel TC. MRS Symp Proc 2003;754:CC7.9.1.
[32] Fang C, Li C, Inoue A. Phys Rev B 2000;61:R3761.
[33] Basu J, Nagendra N, Li Y, Ramamurty U. Philos Mag 2003;83:1747.
[34] Van Den Beukel A, Seitsma J. Acta Metall Mater 1990;38:383.
[35] Slipenyuk A, Eckert J. Scripta Mater 2004;39:44.
[36] Kramer MJ, Sordelet DJ, Bastarows AF, Tan X, Biner SB. J Non-Cryst Solid 2005;351:2159.
[37] Safarik DJ, Cady CM, Schwarz RB. Acta Mater 2005;53:2193.
[38] Jiang WH, Pinkerton FE, Atzmon M. Acta Mater 2005;53:3469.
[39] Yavari AR, Moulec AL, Inoue A, Nishiyama N, Lupu N, Matsubara E, et al. Acta Mater 2005;53:1611.